

Nonlinear Reactance of Superconducting Films*

J. GITTLEMAN, B. ROSENBLUM, T. E. SEIDEL, AND A. W. WICKLUND

RCA Laboratories, Princeton, New Jersey

(Received 3 August 1964)

The dependence of the imaginary part of the conductivity (σ_2) on current has been measured at various temperatures for films of tin, indium, and tin-indium alloys. The samples were thin, narrow films so that both the dc and microwave currents were spatially uniform. The reactance of the samples was measured with a small 23-kMc/sec signal while the direct current in the film was varied from zero to the critical value. At reduced temperatures above 0.6, both the magnitude and the temperature dependence of the nonlinearity were in remarkably good agreement with both the microscopic theory of Parmenter and the phenomenological Ginsburg-Landau theory. The only adjustable parameter was the penetration depth for each sample. The values chosen for the penetration depth were in excellent agreement with values computed from residual resistance ratios. There was also an indication in our data that the boundary scattering in indium films is highly specular, whereas in the tin films it appears to be diffuse.

INTRODUCTION

A CURRENT flowing in a superconductor increases the number of quasiparticle excitations in the superconductor. These excitations cause the high-frequency conductivity of the superconductor to be a function of the current. The consequent nonlinear relationship between the current and electric field in superconductors has been observed earlier¹ and the present paper reports extensions of these studies. Nonlinearities have previously been observed by Nethercot and von Gutfeld² in connection with their studies of the switching time in superconductors by observing the harmonic content of high power microwave signals reflected from the superconductor. Sherrill and Rose³ also reported nonlinearities at microwave frequencies which they associated with switching.

In the present experiment a filamentary geometry is chosen where the sample is narrow enough and thin enough that the direct and microwave current densities are approximately uniform throughout the filament. The inductance of a superconducting filament is measured with a very small microwave current as a function of a much larger direct current through the filament. This is a direct and simple way to study the nonlinearity. In the present experiments we have studied tin, indium, and their alloys.

There are two theoretical approaches to the analysis of our data. The first is the phenomenological theory of Ginsburg and Landau,⁴ which is only derived for temperatures near the transition temperature. It is known,

however, that in many cases its range of validity is surprisingly great. The second theoretical approach is an extension of the BCS theory by Parmenter⁵ to the case of finite currents in superconductors with small coherence distances. We will compare our results with calculations based on each of these theories.

In the London theory⁶ the current density \mathbf{j} is related to the electric and magnetic fields \mathbf{E} and \mathbf{H} by

$$\text{Curl} \mathbf{j} = -(c/4\pi\lambda^2)\mathbf{H} \quad (1)$$

and

$$\partial \mathbf{j} / \partial t = (c^2/4\pi\lambda^2)\mathbf{E}, \quad (2)$$

where λ is the penetration depth. Assuming an $e^{i\omega t}$ time dependence, we may write $\mathbf{j} = -i\sigma_2\mathbf{E}$, where the conductivity σ_2 is given by

$$\sigma_2 = c^2/4\pi\omega\lambda^2 = ne^2/m\omega, \quad (3)$$

where n , e , and m are the number density, charge, and mass of the electrons. Equation (3) is, of course, just the conductivity of a free-electron gas in the limit that the scattering time goes to infinity.

The simple form of the London theory is readily generalized to the two-fluid model which gives an excellent physical picture of high-frequency behavior of superconductors. In this model one considers each electron to be in either the normal or the superconducting state. The same electric field is seen by all the electrons so that they are all essentially "in parallel." Each of the normal electrons is considered to have a resistance $r(=mL/e^2\tau A)$ and an inductance $l(=mL/e^2A)$, where τ is the scattering time in the normal state, L the length of the conductor, and A the cross-sectional area. For the superconducting electrons, $r=0$ and l is the same as for the normal electrons. The equivalent circuit for this two-fluid system is shown in Fig. 1. L_0 is the geometric or magnetic inductance of the superconductor, and n_n the number of electrons in the normal state, and n_s the number in the superconducting state. If $\omega l \ll r$, as is often the case, n in Eq. (3) can be identified with n_s .

* The research reported in this work was sponsored by the Advanced Research Projects Agency (ARPA Order 210-61) contract DA36-039-SC-88959, monitored technically by the U. S. Army Electronics Research and Development Laboratories, Fort Monmouth, New Jersey.

¹ J. Gittleman, B. Rosenblum, T. Seidel, and A. Wicklund, in *Proceedings of the Eighth International Conference on Low Temperature Physics* (Butterworths Scientific Publications, Ltd., London, 1963), p. 336.

² A. H. Nethercot, Jr., and R. J. von Gutfeld, *Phys. Rev.* **131**, 576 (1963).

³ M. D. Sherrill and K. Rose, *Rev. Mod. Phys.* **36**, 312 (1964).

⁴ V. L. Ginsburg and L. D. Landau, *Zh. Eksperim. i Teor. Fiz.* **20**, 1064 (1950).

⁵ R. H. Parmenter, *RCA Rev.* **23**, 323 (1962).

⁶ F. London and H. London, *Proc. Roy. Soc. (London)* **A149**, 71 (1935).

If we neglect the inductive reactance of the normal carriers, it is easily seen that the net inductance increases as the number of normal electrons increases and the number of superconducting electrons decreases. In the two-fluid model of Gorter and Casimir⁷ the fraction of the electrons which are superconducting varies as $1-t^4$, where $t=T/T_c$ the reduced temperature. T is the temperature and T_c the transition temperature. The model does not, however, admit any variation in n_s or σ_2 with current.

The Ginsburg-Landau theory is an extension of the London-Gorter-Casimir approach in which n_s is allowed to vary spacially and is assumed to be proportional to the order parameter $|\Psi|^2$ where Ψ is an effective wave function characterizing the superconducting state. As we shall see, the solution of the Ginsburg-Landau equations yields a dependence of Ψ on the applied magnetic field or current. This, in turn, gives a field and current dependence to the penetration depth and σ_2 . We assume that the samples in the present experiment are sufficiently small that the density of superconducting electrons is uniform.

In the Parmenter theory one notes that when a current is flowing in a superconductor the energy of the electrons at the forward end of the Fermi sphere is higher than the energy of the electrons at the back end by

$$\frac{1}{2}m(v_f+v_d)^2 - \frac{1}{2}m(v_f-v_d)^2 = 2p_f v_d,$$

where v_d is the drift velocity and v_f and p_f are the Fermi velocity and Fermi momentum, respectively. The "optical gap" $2\epsilon_0$, the energy needed to excite quasiparticles with conservation of momentum, is nearly independent of current for currents well below the critical value. However, the energy needed to create quasiparticles by scattering from the front to the back of the Fermi sphere is reduced by $2p_f v_d$. Thus one can define a "thermal-energy gap" $2(\epsilon_0 - p_f v_d)$. This is illustrated in Fig. 2. It is thus readily seen that at any nonzero temperature a current will increase the number of quasiparticles. Because of this excitation of quasiparticles the electric field does more than merely displace the Fermi sphere and the current-field relationship is nonlinear. At a given thermal-energy gap the number of excitations

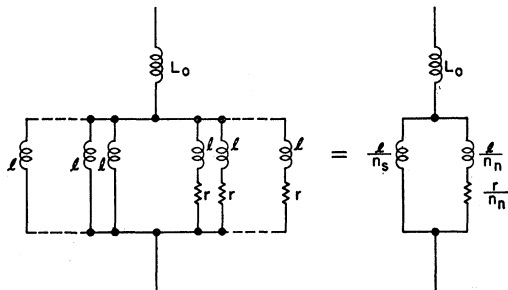


FIG. 1. The two-fluid-model equivalent circuit.

⁷ C. J. Gorter and H. B. G. Casimir, *Physik Z.* **35**, 963 (1934).

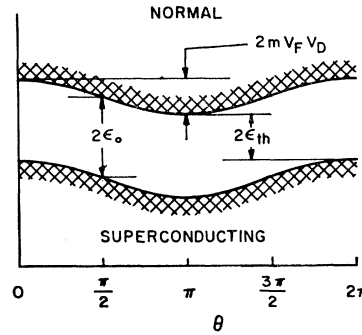


FIG. 2. Energy gap versus direction in a current-carrying superconductor.

must decrease to zero as the temperature goes to zero. Therefore, in the Parmenter theory nonlinearities disappear at very low temperatures.

THEORY

The Ginsburg-Landau Theory

Since the experimental work involves thin films in which the current density is fairly uniform, the Ginsburg-Landau equations are applied to the one-dimensional problem of an infinitely wide slab of thickness $2d$. In this case the equations⁴ become

$$d^2\varphi/d\xi^2 = \kappa^2\{-(1-a^2)\varphi + \varphi^3\}, \tag{4}$$

$$d^2a/d\xi^2 = \varphi^2 a, \tag{5}$$

where

$$a = A/\sqrt{2}H_c\lambda, \quad \varphi = (\lambda/\lambda_0)\psi, \quad \kappa^2 = (2e^2/\hbar^2c^2)H_c^2\lambda^4, \text{ and } \xi = z/\lambda.$$

A = the vector potential,

$|\psi|^2$ = the Ginsburg-Landau order parameter,

H_c = the bulk critical magnetic field,

λ = the weak-field penetration depth,

$\lambda_0^2 = mc^2/4\pi ne^2 = \lambda^2$ at absolute zero, and

z = distance measured perpendicular to the film boundary.

There are two limiting cases for which solutions can readily be obtained. They are for $\kappa=0$ and $\kappa=\infty$. For $\kappa=0$, Ginsburg and Landau give for the solutions:

$$\varphi = \varphi_0, \tag{6}$$

$$a = h_0 \cosh \varphi_0 \xi / \varphi_0 \sinh(\varphi_0 d/\lambda), \tag{7}$$

$$\varphi_0^2(1 - \varphi_0^2) = \frac{1}{2}h_0^2 \times \left[1 + \frac{\sinh(2\varphi_0 d/\lambda)}{2\varphi_0 d/\lambda} \right] / \sinh^2(\varphi_0 d/\lambda), \tag{8}$$

where $h_0 = H_0/\sqrt{2}H_c$ and $H_0 = (4\pi/c)jd$ = the magnetic field at the film surface due to the current density j . For sufficiently thin films,

$$\varphi^2 = 1 - (\lambda/d)h_0^2 = 1 - (8\pi^2/c^2)(\lambda d/H_c^2)j^2. \tag{9}$$

For $\kappa = \infty$, $(1/\kappa^2)(d^2\varphi/d\xi^2) = 0$ and

$$\varphi^2 = 1 - a^2, \quad (10)$$

and

$$a = h_0 \cosh \xi / \sinh(d/\lambda) \quad \text{for } a^2 \ll 1. \quad (11)$$

So for sufficiently thin films,

$$\varphi^2 = 1 - (8\pi^2/c^2)(\lambda/H_c)^2 j^2. \quad (12)$$

Putting $\lambda^2 = \lambda_0^2(1-t^4)^{-1}$ and $H_c = H_0(1-t^2)$, where $t = T/T_c$:

for

$$\kappa = 0, \quad |\psi|^2 = \left(\frac{\lambda_0}{\lambda}\right)^2 \left[1 - \frac{8\pi^2 \lambda_0 d}{c^2 H_0^2} f_0(t) j^2\right]; \quad (13)$$

for

$$\kappa = \infty, \quad |\psi|^2 = \left(\frac{\lambda_0}{\lambda}\right)^2 \left[1 - \frac{8\pi^2 \lambda_0^2}{c^2 H_0^2} f_\infty(t) j^2\right]; \quad (14)$$

where

$$f_0 = (1-t^2)^{-2}(1-t^4)^{-1/2} \quad \text{and} \quad f_\infty = (1-t^2)^{-2}(1-t^4)^{-1}.$$

The Ginsburg-Landau expression for the current is

$$\mathbf{j} = -(c/4\pi\lambda_0^2) |\psi|^2 \mathbf{A} = -(c/4\pi\lambda^2) [1 - k^2(\kappa) j^2] \mathbf{A}, \quad (15)$$

where

$$k^2 = (8\pi^2/c^2)(\lambda_0 d/H_0^2) f_0(t) \quad \text{or} \quad (8\pi^2/c^2)(\lambda_0^2/H_0^2) f_\infty(t)$$

for

$$\kappa = 0 \quad \text{or} \quad \infty.$$

Putting $j = j_{dc} + j_{ac}$, where $j_{ac} \propto e^{i\omega t}$ and is small compared with j_{dc} and noting that $E_{ac} = -(1/c)(\partial A/\partial t)$ we obtain

$$j_{ac} = (c^2/4\pi i \omega \lambda^2) [1 - 3k^2(\kappa) j^2] E_{ac}. \quad (16)$$

Thus⁸

$$\sigma_2(j, t) = (c^2/4\pi \omega \lambda^2) [1 - 3k^2(\kappa) j^2]. \quad (17)$$

As will be discussed later, the measurements are proportional to the fractional change of σ_2 . So that

$$\left[\frac{\sigma_2(0, t) - \sigma_2(j, t)}{\sigma_2(0, 0)} \right]_{\kappa=0} = \frac{24\pi^2 \lambda_0 d}{c^2 H_0^2} g_0(t) j^2, \quad (18)$$

and

$$\left[\frac{\sigma_2(0, t) - \sigma_2(j, t)}{\sigma_2(0, 0)} \right]_{\kappa=\infty} = \frac{24\pi^2}{c^2} \left(\frac{\lambda_0}{H_0}\right)^2 g_\infty(t) j^2, \quad (19)$$

where

$$g_0(t) = (1-t^4)^{1/2}(1-t^2)^{-2} \quad \text{and} \quad g_\infty(t) = (1-t^2)^{-2}.$$

The Parmenter Theory

When the Cooper pairs have a net velocity \mathbf{v}_0 , Parmenter⁵ shows that quasiparticle excitations in ex-

⁸ It should be noted that it has been assumed that ψ^2 can freely follow the ac field. If ψ^2 is rigid in time, then $\sigma_2(j, t) = (c^2/4\pi\lambda^2) \times [1 - k^2 j^2]$. In the Parmenter theory, which is treated in the following section, the same reduction of the coefficient of j^2 is obtained if the assumption of rigidity is assumed.

cess of the zero-current thermal excitations will exist. These excitations have a mean velocity \mathbf{v}_Q , which is opposite to \mathbf{v}_0 such that $\mathbf{v} = \mathbf{v}_0 + \mathbf{v}_Q$ and $\mathbf{j} = ne\mathbf{v}$, the net current of the superfluid. The existence of this contribution to the current was first suggested by Bardeen.⁹ The quasiparticle contribution is given by

$$\mathbf{v}_Q = (3/p_F) \int_0^\infty Q[\beta E, \beta p_F v_0] d\epsilon, \quad (20)$$

$$Q(a, b) = \frac{1}{2} \int_{-1}^{+1} \mu \left[1 - \tanh\left(\frac{a+b\mu}{2}\right) \right] d\mu, \quad (21)$$

where

p_F = the Fermi momentum,

$$\beta = 1/kT,$$

$$E = \{\epsilon^2 + \epsilon_0^2\}^{1/2},$$

$2\epsilon_0$ = the superconducting energy gap.

If \mathbf{v}_Q is expanded in powers of v_0 , \mathbf{v} becomes

$$\mathbf{v} = \gamma_1(T) \mathbf{v}_0 - (1/20) \beta^2 p_F^2 \gamma_2(T) v_0^3 \quad (22)$$

omitting terms of the order of v_0^5 and higher.

$$\gamma_1(T) = 1 - \frac{1}{2} \beta \int_0^\infty \text{sech}^2(\beta E/2) d\epsilon \quad (23)$$

which is the BCS expression for the London parameter¹⁰ $\Lambda(0)/\Lambda(T)$ and

$$\gamma_2(T) = \beta \int_0^\infty [\text{sech}^2(\beta E/2) - \frac{3}{2} \text{sech}^4(\beta E/2)] d\epsilon. \quad (24)$$

In the Parmenter theory, $\mathbf{j}_0 = -ne^2 \mathbf{A}/mc$ where $\mathbf{j}_0 = ne\mathbf{v}_0$. Thus if we calculate $\sigma_2(0, t) - \sigma_2(j, t)$ by putting $j_0 = j_{0dc} + j_{0ac}$ and proceed as for the Ginsburg-Landau theory, we get

$$[\sigma_2(0, t) - \sigma_2(j, t)]/\sigma_2(0, 0) = (3/20) \beta^2 p_F^2 \gamma_2(t) v_0^2, \quad (25)$$

where

$$\sigma_2(0, t) = \sigma_2(0, 0) \gamma_1(t),$$

omitting terms in v_0^4 and higher. To this degree of approximation we can put $\mathbf{v} = \gamma_1(t) \mathbf{v}_0$ so that

$$\frac{\sigma_2(0, t) - \sigma_2(j, t)}{\sigma_2(0, 0)} = \frac{3}{20} \frac{p_F^2}{n^2 e^2 k^2 T_e^2} \left[\frac{\gamma_2(t)}{t^2 \gamma_1^2(t)} \right] j^2. \quad (26)$$

In the above calculation it has been assumed that ϵ_0 is independent of v_0 . This is not true in the Parmenter theory. However, in view of the fact that ϵ_0 is an even function of v_0 , the results are formally unchanged if

⁹ J. Bardeen, Phys. Rev. Letters **1**, 399 (1958).

¹⁰ J. Bardeen, L. N. Cooper, and J. R. Schrieffer, Phys. Rev. **108**, 1175 (1957).

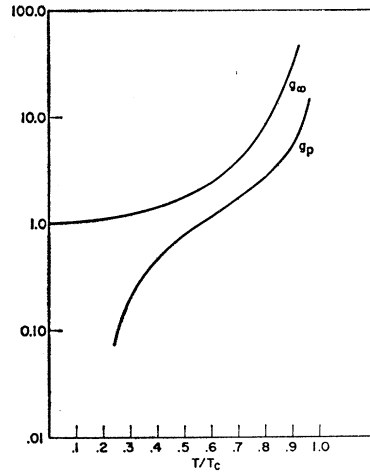


FIG. 3. The Ginsburg-Landau function ($\kappa = \infty$) and the Parmenter function versus reduced temperature.

$\gamma_2(T)$ is modified to be

$$\gamma_2(T) = \beta \int_0^\infty \left\{ \left[1 - \frac{5\epsilon_0}{\beta E} \frac{d^2\epsilon_0}{d(p_F v_0)^2} \right] \times \operatorname{sech}^2(\beta E/2) - \frac{3}{2} \operatorname{sech}^4(\beta E/2) \right\} d\epsilon,$$

where $d^2\epsilon_0/d(p_F v_0)^2$ is evaluated at $v_0 = 0$. Over the temperature range of experiment, at least, this correction is negligible. As T approaches T_c $\epsilon_0[d^2\epsilon_0/d(p_F v_0)^2]$ tends toward zero, although near T_c there may be a contribution to the integral for values of ϵ_0 near zero. This has not been calculated.

Parmenter⁵ shows that $p_F v_c(0) = 1.011 p_F v_{00} = 1.011 \epsilon_0$, where $n e v_c(0)$ is the maximum current density in a superconductor at $T = 0^\circ\text{K}$. Thus we put $j_c(0) = n e v_c(0)$ = the critical current at absolute zero. Then the current dependence of σ_2 takes the form

$$\frac{\sigma_2(0, t) - \sigma_2(j, t)}{\sigma_2(0, 0)} = \frac{3}{20} (1.011)^2 \times \left[\frac{\epsilon_0}{k T_c} \right]^2 \left[\frac{\gamma_2(t)}{t^2 \gamma_1^2(t)} \right] \frac{j^2}{j_c(0)^2}. \quad (27)$$

But $\epsilon_0/kT_c = 1.75$ from the BCS theory and Bardeen¹¹ points out that $\frac{1}{2}[4\pi\lambda_0^2/c^2]^2[\frac{3}{2}j_c^2(0)] = H_0^2/8\pi$ so that $j_c^2(0) = \frac{1}{3}(c^2/8\pi^2)(H_0^2/\lambda_0^2)$. Finally, therefore, the change in σ_2 becomes

$$\frac{\sigma_2(0, t) - \sigma_2(j, t)}{\sigma_2(0, 0)} = \frac{24\pi^2}{c^2} \left(\frac{\lambda_0}{H_0} \right)^2 g_p(t) j^2, \quad (28)$$

$$g_p(t) = \frac{1.38}{3} \frac{\gamma_2(t)}{t^2 \gamma_1^2(t)}.$$

In the limit of $t = 0$, $g_p(0) = 0$ whereas $g_\infty(0) = 1$. However, inasmuch as the Ginsburg-Landau theory is a

high-temperature theory, not much significance should be given to its behavior near absolute zero. Near $t = 1$,

$$g_\infty \propto (1-t)^{-2}$$

whereas

$$g_p \propto (1-t)^{-1}.$$

Thus, even near the critical temperature, a difference exists between the two theories. The integral of Eq. (24) was evaluated numerically, and Fig. 3 is a plot of g_∞ and g_p as a function of reduced temperature. It is noted that in the temperature range to which the experiments were confined ($0.3 < t < 0.95$) the nonlinearities predicted by the two theories are of the same order of magnitude. Except very near $T = T_c$, g_0 is very nearly equal to g_∞ and has not been plotted.

That the results from the Ginsburg-Landau theory differ from those from Parmenter's theory even near T_c is implicit in Ref. 5. It is pointed out that the Ginsburg-Landau equations may be obtained from the Parmenter theory if the order parameter $|\psi|^2$ is associated with v/v_0 , provided

$$v = \gamma_1(T) v_0 - \frac{1}{2} [\gamma_1^2(T)/v_c^2] v_0^3,$$

where

$$\frac{1}{2} n m v_c^2 = H_c^2/8\pi.$$

This is similar to the expansion obtained earlier for $v(v_0)$ [Eq. (22)]. In fact the first term is identical. However, the difference in the temperature dependence of the coefficients of v_0^3 correspond exactly to the differences noted between g_p and g_∞ .

EXPERIMENTAL

Since there is a nonlinear relationship between current and electric field in a superconductor, the ac impedance of the superconductor will depend on the current. The nonlinear behavior can then be studied by measuring the impedance with a very small ac signal as the direct current in the superconductor is varied.

The supercurrent changes the inductance of the specimens used by about 10^{-12} henry. Since this inductance change is due to the change in the effective mechanical inertia of the carriers, it cannot be increased by extra flux linkages as is the case for the usual magnetic inductance. The inductance is proportional to the length of the superconductor, but it is not practical to make our specimens more than a few millimeters long. The total inductance of the specimen was about 10^{-9} henry. To measure such small inductances it is appropriate that the ac signal be at microwave frequencies. The microwave photon energy should, however, be smaller than the superconducting energy gap at any of the temperatures of measurement. Unlike the inductance, the real part of the impedance increases with frequency. In the present case, even at these very high frequencies the real part is small compared to the imaginary part, and only the inductance change was experimentally studied.

¹¹ J. Bardeen, Rev. Mod. Phys. 34, 667 (1962).

In order to be able to obtain quantitatively meaningful results, it is important that the direct current density be approximately uniform throughout the sample. This will be the case if the sample is sufficiently small in dimensions perpendicular to the current flow. The samples were therefore thin, narrow films on glass or quartz substrates. These were mounted so that the sample formed an inductive post, parallel to the electric field, in a rectangular TE_{01n} cavity which resonated at about 23 kMc/sec. The cavity terminated one arm of a microwave bridge. The change in the inductance was determined by the change in the resonant frequency of the cavity.

The problem of a thin post of arbitrary impedance across a waveguide closed at both ends is treated by Slater.¹² If one adds the impedance of the post to his Eq. (40.6), one obtains the total impedance of the cavity as seen from a particular set of terminals. The resonant frequency is independent of the particular terminals of observation, and one can find this frequency by equating the imaginary part of the impedance to zero. However, since the frequency changes are small and are caused by small changes in the post reactance,

$$d\omega = FdX,$$

where ω is the resonant frequency, X is the imaginary part of the impedance of the post, and F is a constant which depends on the cavity dimensions, position and dimensions of the post, and frequency, but is independent of current and temperature. We have assumed that $dX \ll X$. The value of F could be obtained in principle from the Slater treatment.

From comparison with the theory we wish to relate X to the complex conductivity of the superconductor. We may write the impedance of the post Z as the series combination of the geometric inductive reactance X_0 and the impedance Z_s due to the scattering and the inertia of the electrons in the superconductor: $Z = iX_0 + Z_s = iX_0 + 1/Y_s$, where the admittance of the electrons is $Y_s = (\sigma_1 - i\sigma_2)A/l$, and σ_1 and σ_2 are the real and the imaginary parts of the electronic conductivity, A is the area, and l is the length of the post. We assume the post is sufficiently thin to be uniformly penetrated by the microwave field. We then have

$$X = X_0 + (l/A)[\sigma_2/(\sigma_1^2 + \sigma_2^2)] \approx X_0 + (l/A)(1/\sigma_2), \quad (29)$$

$$d\omega = FdX = -(l/A)F(d\sigma_2/\sigma_2^2), \quad (30)$$

where we have assumed that $\sigma_2^2 \gg \sigma_1^2$, $X_0 \gg (l/A)(1/\sigma_2)$, and $\sigma_2 \gg d\sigma_2$ which are excellent approximations except extremely close to the transition temperature or the critical current.

The experimentally measured quantity is $d\omega(j,t)$ whereas the desired quantity is $d\sigma_2(j,t)$. Thus to compare with theory F must be determined. Although it is

¹² J. C. Slater, *Microwave Transmission* (McGraw-Hill Book Company, Inc., New York, 1946), p. 300.

impractical to compute the value of F for the actual nonideal cavity configuration used in the experiment, an effective value may be obtained by measuring the shift in the cavity resonant frequency with temperature at zero current. By assuming that $\sigma_2(0,t)$ is that given by BCS, one can determine the $\sigma_2(j,t)$ itself absolutely, and not just its dependence on j and t .

The signal S traced by the recorder pen is proportional to the changes in cavity frequency. For the case where the current is square-wave modulated and the temperature is constant, Eq. (30) becomes

$$S_j = \omega(j,t) - \omega(0,t) = \frac{lF}{A} \frac{\sigma_2(0,t) - \sigma_2(j,t)}{\sigma_2^2(0,t)}, \quad (31)$$

where we have written differences rather than differentials, with the understanding that the differences are small. At zero current the temperature is raised, keeping all other system parameters unchanged from the measurement of S_j . The fractional changes in σ_2 in this case are not necessarily small, but since the fractional changes in ω and X are small, Eq. (30) can be used. Therefore,

$$S_t = \omega(0,t_1) - \omega(0,t_2) = \frac{lF}{A} \frac{\sigma_2(0,t_2) - \sigma_2(0,t_1)}{\sigma_2(0,t_2)\sigma_2(0,t_1)}. \quad (32)$$

Since S_t is measured and $\sigma_2(0,t)$ is calculated from theory, lF/A is determined. Thus $\sigma_2(j,t)$ can be computed from the measured S_j .

Samples

To have the current distribution uniform throughout the sample it is necessary that the thickness be small compared to the penetration depth and that the width not be very large. The penetration depth in the film is expected to be larger than for the bulk material and a typical value (chosen to fit the experimental data) was 2000 Å. The film thickness was about 500 Å. This ratio of four should insure a sufficiently uniform distribution through the film thickness. The width of the film must be small enough that the crowding of the flux lines around the film edge does not produce a nonuniform distribution across the width. The samples were less than 15 μ wide. Roughly extrapolating the results of Marcus,¹³ we believe the current to be reasonably uniform.¹⁴ This conclusion is supported by the fact that

¹³ Paul M. Marcus, *Proceedings VII International Conference on Low Temperature Physics, Toronto, Canada*, edited by G. M. Graham and A. C. Hollis Hallett (University of Toronto Press, Toronto, 1961), p. 418.

¹⁴ Instead of using an extremely narrow thin film one could insure uniformity by evaporating a thin film on a circular cylinder. However, if the diameter of the cylinder were very small it would not be possible to cool the substrate during evaporation. If it were larger, the fractional change in the inductance would be much smaller since the inductance due to electronic inertia is inversely proportional to the film radius while the geometric inductance varies logarithmically. The current required also becomes inconveniently large for a cylinder as large as 1 mm in diameter.

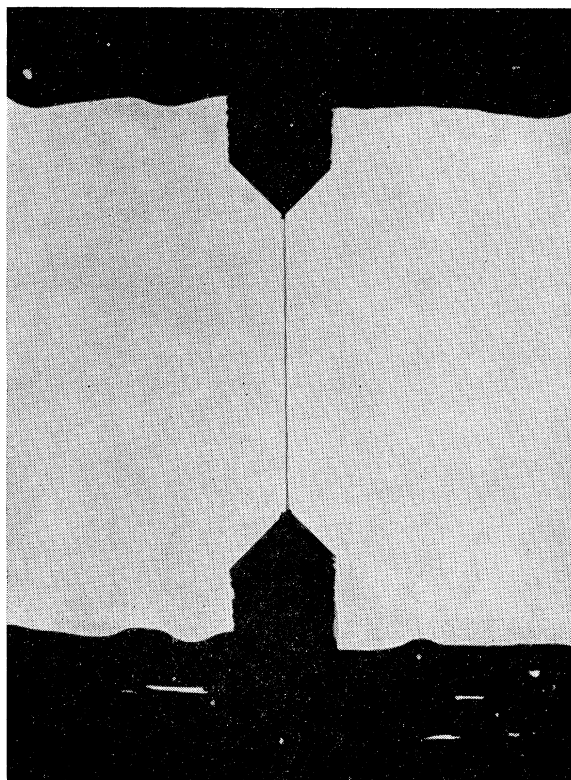


Fig. 4. Microphotograph of specimen.

samples with widths differing by more than a factor of 4 give similar results.

A microphotograph of a sample is shown in Fig. 4. The substrates were optically polished glass plates 0.400 in. \times 0.200 in. \times 0.0025 in. Platinum soldering tabs were baked on each end of the substrate. The sample metal was evaporated to form thin strips 2 mm long and nominally 7×10^{-4} cm wide and 500 Å thick, the last two dimensions varying among samples. In order to minimize current density changes along the same strip, samples with deviations from mean width of the film greater than 10% were rejected. The ends of the narrow sample strip were wide to provide good contact to the platinum tabs. The platinum tabs and the sample metal on the ends were then covered by several thousand angstroms of evaporated lead to insure a completely superconducting current path to eliminate resistive heating by the applied currents, which reached 30 mA.

The samples were evaporated through special masks of 0.0002-in.-thick electroformed nickel provided by RCA Electron Tube Division, Lancaster, Pennsylvania. Because of the extreme thinness of the masks, care was needed to insure the parallel alignment of edges to $\pm 5 \times 10^{-5}$ cm. The mask and substrate were sandwiched tightly between a copper plate, slotted to leave the mask center open, and a spring-loaded quartz block. This sandwich was mounted in a copper block which was, in turn, bolted directly to the bottom of a liquid-

nitrogen can in a vacuum system. All evaporations were made at pressures of about 3×10^{-6} mm Hg with the substrates cooled to near liquid-nitrogen temperatures. Evaporation boats were tantalum cones cemented to molybdenum helically wound boats with a high-temperature silicate cement. The alloy films were from an alloy evaporand, which was prepared by melting together under high vacuum the approximate proportion of constituents desired in the film. Since the constituents possessed differing vapor pressures, the resulting films were rich in the more volatile constituent and it was necessary to spectrographically analyze a film prepared coincidentally with the sample. All films used were clean and free from any blemish when inspected with an 800 \times microscope. The penumbra was always an extremely small fraction of the approximately 7μ width.

To determine the film thickness, the residual resistance at 4.2°K was subtracted from the room-temperature resistance and the difference was taken to be the room-temperature thermal resistance without imperfection and boundary scattering. With this resistance and the other dimensions of the film, bulk resistivity values were used to compute the thickness. The thickness was also determined by measuring interferometrically the thickness of a specimen made in the same evaporation as the sample. In our thickness range, the two methods were in fair agreement.

Before the samples were mounted in the microwave cavity they were lightly coated with GE-7031 varnish. The samples were then mounted through 0.015-in. slots cut through both walls of the constricted portion of the cavity. The lead covered platinum tabs projected from the slots leaving only the central strip of the film within the microwave field. Our projecting tab rested on a shelf which is an integral part of the outer wall of the cavity. The sample was fixed rigidly to this shelf by GE-7031 varnish or Hysol Epoxi-Patch. All wires to the sample were superconducting for the final 4 in. of their length to eliminate any heating in the neighborhood of the film. Solid lead wires were used, with the final connection to the sample being made by lead plated No. 40 copper wire.

Experimental Technique

The inset in Fig. 5 shows a simplified cross section of the microwave cavity showing the mounted sample. The cavity was usually operated in a TE₀₁₇ mode. In the region of the sample the cavity was narrowed in the direction of the microwave electric field so that only the narrow part of the film would be in a region of appreciable microwave field. The cavity was made by electroforming copper on an aluminum mandrel. It was found convenient to mount the sample a considerable distance from an antinode of electric field. This reduced the signal-to-noise ratio, but allowed observation of the cavity resonance, even when the sample was normal.

The sensitivity of the system could be adjusted by changing the operating frequency and retuning the cavity, thus changing the distance of the sample from the antinode of electric field. There was some small loss of microwave power by radiation through the mounting slot, the sample acting as an antenna. This, however, did not greatly affect the Q of the cavity which was approximately 3000.

The cavity was soldered to the waveguide and enclosed in a vacuum tight can which was immersed in the liquid helium. The can contained helium gas at a pressure of a fraction of a mm Hg to act as a thermal conductor between the sample and the bath. The temperature of the cavity assembly was monitored with a carbon resistance thermometer. A heater attached to the cavity allowed the temperature of the cavity assembly to be varied independently of the external helium-bath temperature. In measurements of σ_2 versus current the heater was not used for measurements below 4.2°K. Instead, the temperature was that of the helium bath. This latter was controlled by an automatic temperature regulating system.

Figure 5 is a schematic diagram of the microwave system and a simplified block diagram of the electronics. The waveguide into the Dewar is kept as short as consistent with the cryogenic requirements in order to minimize the "long-line" reflections. The matched hybrid tee was fastened directly to the waveguide leaving the Dewar for the same reason.

The microwave power incident on the cavity was always less than $1 \mu\text{W}$, and the sample was positioned in a moderately low-field region of the cavity. The microwave current in the sample therefore did not contribute significantly to the nonlinearity but merely served as a probe to measure the inductance. This was verified by noting that the measured inductance was independent of the microwave power, except extremely close to the critical current.

The change in frequency of the cavity when the sample was driven with a current close to critical current was of the order of 1% of the cavity resonance width. A plot of the frequency change versus current

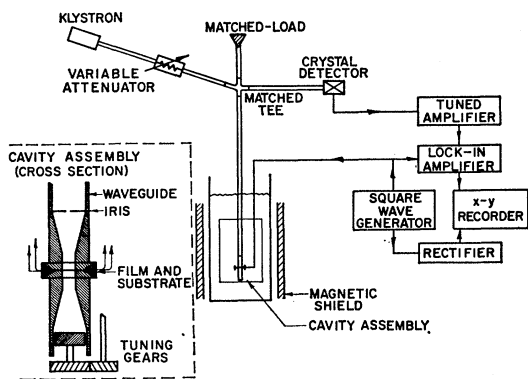


FIG. 5. Schematic diagram of apparatus.

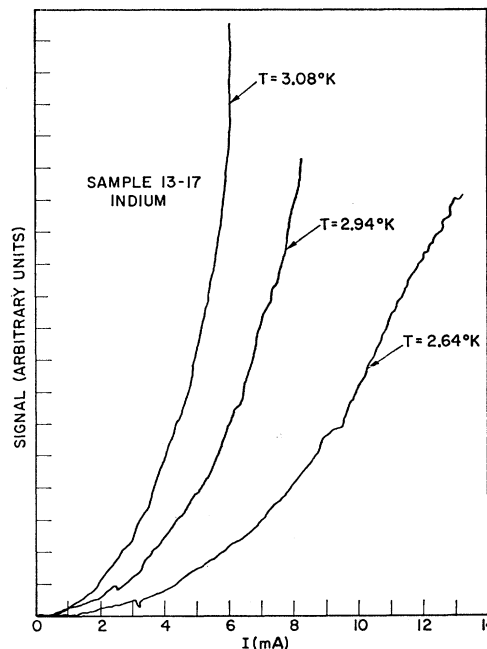


FIG. 6. Microwave signal versus sample current.

was obtained on an x - y recorder in the following manner: The current to the sample was supplied by a square-wave generator. The zero-based square-wave generator switched the current from on to off at 1000 cps. The klystron was tuned to the frequency of one of the inflection points in the plot of power reflected from the cavity versus frequency. At such a point the change in reflected power for a given change in cavity frequency is a maximum. The 1000-c/sec change in reflected power resulting from the square-wave current in the sample was detected by the crystal, and fed to a tuned 1000-c/sec amplifier. This amplified signal was in turn fed to a lock-in amplifier which mixed the signal with a reference signal derived from the square-wave generator. The output of the lock-in, which had a bandwidth of about 1 sec, was then displayed on the y axis of the x - y recorder. The x axis of this recorder was driven by a dc voltage proportional to amplitude of the square wave of current through the sample.

To calibrate the system so that the measured frequency change could be related to an impedance change, the shift in cavity frequency at zero current was measured when the temperature was changed from a value well below the critical temperature to one near the critical temperature. This frequency change was large enough that it could be measured by directly observing the shift of the cavity resonance displayed on an oscilloscope by sweeping the klystron frequency. For this observation the temperature was varied by adjusting the current in the heater mounted on the cavity assembly. This is not a very accurate technique and in some cases limited the absolute accuracy of our measurement to about 50%.

TABLE I. Sample data summary.

Sample No.	Material	Width μ	Thickness \AA	$\frac{R_{300}}{R_4}$	λ_0 (\AA)		
					Parmenter	Ginsburg-Landau	Calculated
14-1	Tin	3.0	525	4.3	1780	1130	1400
13-6	Tin	13.0	540	5.7	4000	2350	1170
7-4	Tin	13.0	250	4.6	1700	1600	1350
13-7	Tin+2½% In (Approx.)	12.5	550	1.25	5400	4130	5000
13-10	Tin+2% In (Approx.)	12.5	260	2.5	3500	2500	2100
13-14	Indium	13.0	380	12.7	770	400	1000
1-2	Indium	5.0	480	10.3	660	400	1100

Magnetic shields of Netic and Conetic were wrapped around the outside of the Dewar to shield the sample from the Earth's magnetic field. It was found that magnetic fields as small as 0.1 G significantly affected our results. This magnetic effect is the subject of continued investigation.

DISCUSSION AND RESULTS

Figure 6 shows typical recorder traces of the signal or shift in cavity frequency as a function of the current at several temperatures. The signal increases somewhat faster than the square of the current. This is as expected from both the Ginsburg-Landau and Parmenter theories.

The theoretical treatment above considered nonlinearities only to terms in j^2 . It is convenient, therefore, to assume that our signal S_j has the form $S_j = A(t)j^2 + B(t)j^4 + \dots$. To obtain $A(t)$ we plot S_j/j^2 as a function of j^2 and extrapolate the curve to zero j^2 . In order to compare the theoretical expression $[\sigma_2(0,t) - \sigma_2(j,t)]/\sigma_2(0,0)j^2$ with the measured $A(t)$, the temperature dependence for $\sigma_2(0,t)$ is needed. When comparing the

data to the Ginsburg-Landau theory we set

$$\sigma_2(0,t) = \sigma_2(0,0)(1-t^4),$$

and when comparing with the Parmenter theory we set

$$\sigma_2(0,t) = \sigma_2(0,0)\gamma_1(t).$$

In order to compare the experiment with each of the theories, the value of the penetration depth at absolute zero λ_0 for each sample was considered as an adjustable parameter. For each sample a value of λ_0 was chosen for best fit to each of the theories. The values used for H_0 were the published bulk values for tin and indium with the tin values used for the alloys.

Table I is a summary of the properties of specimens and values chosen for λ_0 . To compare the experimental data with the theories, the measured values of $\Delta\sigma_2$ were normalized by dividing by the appropriate value of $(24\pi^2/c^2)(\lambda_0/H_0)^2$ and plotted as a function of reduced temperature t . Figure 7 is a plot for the Parmenter theory. The solid curve is the function $g_p(T/T_c)$ which was calculated from theory. Figure 8 is a similar plot for the Ginsburg-Landau theory with $\kappa = \infty$.¹⁵

In the temperature range above $t=0.6$, where the nonlinearities are relatively large, both the magnitude and the temperature dependence can be brought into agreement with either theory with a single adjustable parameter, the penetration depth λ_0 . The values chosen for λ_0 to bring the experiment into agreement with each theory do not differ greatly from each other and indeed are in good agreement with those calculated from the dc resistance ratio (R_{300}/R_4) in the normal state. Since the systematic error in the absolute calibration of our signal may be as high as 50%, the value of the penetration depths chosen for a best fit to each theory cannot form a basis for a preference between them.

The values of λ_0 labeled "calculated" in Table I were obtained from equations discussed by Pippard,¹⁶

¹⁵ Comparison with the case $\kappa=0$ is not shown. The values of λ_0 required to fit the data was much less than for the $\kappa=\infty$ case and the temperature dependence was indistinguishable in the experimental range. Indium was the exception. In this case the same values of λ_0 were obtained for $\kappa=0$ and $\kappa=\infty$.

¹⁶ A. B. Pippard, Proc. Roy. Soc. (London) A216, 547 (1953).

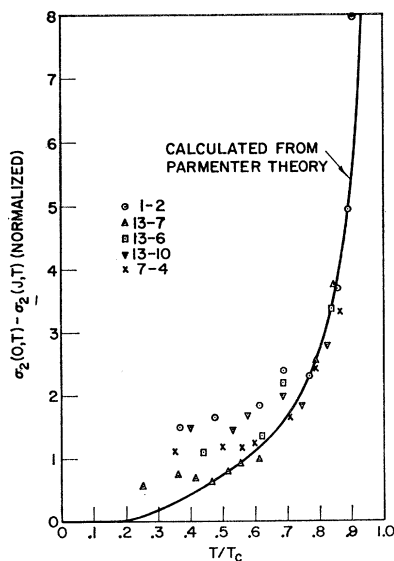


FIG. 7. Comparison of experimental data with Parmenter theory.

Tinkham,¹⁷ and Douglass.¹⁸ Thus λ_0 is given by

$$\lambda_0 = \lambda_B (\xi_0 / \xi)^{1/2},$$

λ_B = the penetration depth for the bulk (pure) material at $T = 0^\circ\text{K}$,

ξ_0 = the Pippard coherence distance,

$$1/\xi \approx 1/\xi_0 + 1/l,$$

where

l = the electron mean free path.

The values for λ_B and ξ_0 are those listed by Lynton.¹⁹ The mean free path was calculated from the residual resistance ratio and the values of ρl listed by Olson.²⁰ The calculated electron mean free paths for the tin films containing the indium impurities were less than 100 Å and far less than the film thickness. This is reasonable if the indium atoms were the dominant electron scatterers, as expected. The mean free paths for the pure tin films were about equal to or somewhat less than the film thickness. Thus the coherence distance for the tin films seems to be dominated by the scattering from the boundary. Boundary scattering from our tin films, therefore, seems to be largely diffuse, although strains or some unknown impurity which is accidentally present in all specimens have not been ruled out.

As can be seen in Table I, the residual resistance ratios of the indium films are considerably greater than the ratios for the others. These ratios lead to mean free paths which are large compared with the film thickness. Thus boundary scattering in indium films appear to be highly specular in contrast with the tin films. The same inference can be drawn from the values of λ_0 obtained by fitting the microwave data. The conclusion concerning the indium films is consistent with results obtained by Serin²¹ from measurements of the penetration of transverse magnetic fields into indium films.

At temperatures below about $t = 0.5$ the nonlinearity predicted by the Parmenter theory decreases rapidly. This is best seen in the logarithmic plot of Fig. 3. This rapid decrease would be expected from any theory in which the mechanism for the nonlinearity is the thermal excitation of quasiparticles. There is a systematic departure from the Parmenter theory for temperatures below about $0.6 T_c$ for all of the specimens. Below about $0.4 T_c$ the nonlinearity becomes temperature insensitive for all specimens. For the specimens of Table I the lowest temperature at which measurements were made was about $0.3 T_c$. However, some lead specimens, from which uncalibrated data were obtained, exhibited tem-

perature independent signals down to $0.17 T_c$. Unfortunately the rapid oxidation of the lead films produced erratic results and prevented us from obtaining data as good as those obtained for tin, indium, and their alloys. It may be noted that this temperature-independent nonlinearity is predicted by the Ginsburg-Landau theory. However, there is no reason to believe this theory to have validity in predicting the nonlinearity at low temperature, and we are inclined to seek the source of the excess low-temperature signal in the "experimental problem" or in an over simplification in the microscopic theory. Maki²² has also considered currents in short coherence distance superconductors. In his treatment nonlinearity remains at $T = 0$ for currents considerably less than the critical value. This is due to the vanishing of the "thermal gap" at about half the critical current. But this theory, too, becomes linear in the limit of zero current and cannot explain the observed low-temperature nonlinearity.

Evaporated films, particularly those of the soft metals with thicknesses under 1000 Å, are generally treated with suspicion. Might the temperature-independent signal be due to "dirt" or oxides which formed a myriad of tiny junctions as the islands of tin grew together when the film was deposited? These junctions, carrying Josephson currents, might cause a nonlinear behavior. One should also keep in mind that the Parmenter theory assumed that the superconductor had a spherical Fermi surface. The actual metals have extremely complicated Fermi surfaces. If, in each of these metals, there were a group of electrons whose thermal-energy

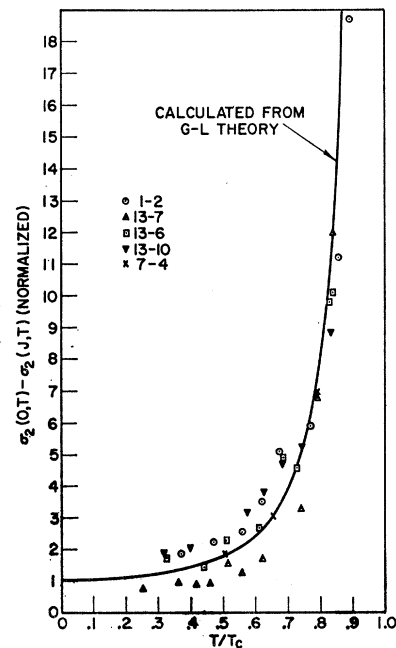


FIG. 8. Comparison of experimental data with the Ginsburg-Landau theory.

¹⁷ M. Tinkham, Phys. Rev. **110**, 26 (1958).

¹⁸ D. H. Douglass, Jr., and R. H. Blumberg, Phys. Rev. **127**, 2038 (1962).

¹⁹ E. A. Lynton, *Superconductivity* (Methuen & Company, Ltd., London, 1962), pp. 5 and 63.

²⁰ J. L. Olsen, *Electron Transport in Metals* (Interscience Publishers, Inc., New York, 1962), p. 84.

²¹ B. Serin (private communication).

²² K. Maki, Progr. Theoret. Phys. (Kyoto) **29**, 333 (1963).

gap was much smaller than the average value (or perhaps even zero), such a temperature-independent nonlinearity at those low reduced temperatures would be expected. The small thermal gap could result from a smaller optical gap for this group of carriers or from a very large Fermi momentum. In any event the temperature-independent nonlinearity is small compared to the nonlinearities at higher reduced temperatures.

In summary, the following conclusions may be drawn from these measurements:

(1) In a local superconductor, $\sigma_2(j, t)$ decreases with increasing current and temperature. From $0.6 T_c$ to the highest temperature at which measurements were made (approx $0.9 T_c$), the current and temperature dependence of the present data agreed remarkably well both with Parmenter's microscopic theory and the Ginsburg-Landau theory. If a conclusion about the differences between the two theories is to be drawn from experiment, the measurements will have to be extended to higher temperatures, or their precision will have to

be increased, or both. Below $0.6 T_c$ the nonlinearity does not decrease as rapidly as predicted by Parmenter.

(2) The values of λ_0 determined from fitting the data to theory, and the measured residual resistance ratios suggest that boundary scattering is more specular in the indium films than in the tin films.

(3) It is interesting to note that if ψ in the Ginsburg-Landau theory, and v_a in the Parmenter theory were assumed to be rigid in the microwave field, that the values of λ_0 would have been larger than the given ones by a factor of $\sqrt{3}$. Thus, calculated electron mean free paths would have been smaller by a factor of 3. For tin and the alloys this appears to us to be quite unreasonable. Therefore, using the nomenclature of Ginsburg and Landau, the order parameter can follow an ac field up to frequencies of 25 kMc or more.

ACKNOWLEDGMENTS

We are grateful to R. H. Parmenter and W. H. Cherry for many valuable and helpful discussions.

Theory of Optical Frequency Mixing Using Resonant Phenomena*

A. JAVAN AND A. SZÖKE†

Physics Department, Massachusetts Institute of Technology, Cambridge, Massachusetts

(Received 11 September 1963; revised manuscript received 31 August 1964)

The nonlinear interaction of two intense optical waves with three energy levels of an atomic system is analyzed theoretically. The frequencies of the applied fields are assumed to be on or near two of the resonances involving the three levels. Particular attention is given to the generation of power at the difference frequency of the two applied fields where their frequency separation lies in the far-infrared range of the spectrum. In the limit of large input fields where atomic transitions are driven to saturation, the generated difference-frequency power is no longer proportional to the product of the two input powers. It is shown that, in this limit, the total rate of emission of photons at the difference frequency may, in principle, approach a value given by rN/T , where N is the total number of atoms, T is the average time of coherent interaction of atoms and the radiation field, and r is a factor which in favorable cases approaches unity at low temperatures. Also, a number of additional effects are encountered due to coherent double-quantum transitions among various levels which may be ignored only for weak input powers. These effects are highly dependent on the modes of relaxations of atomic levels and the details of the line shape. The results are applied to several cases, in which the resonance condition yields large efficiency in nonlinear frequency mixing.

I. INTRODUCTION

THE generation of power at the sum or difference frequency of two optical waves by a nonlinear medium may be described in terms of multiple quantum transitions due to interactions of the incident fields with energy levels of the mixing material. If the frequencies of all the interacting fields are far removed from the resonance transitions of the mixing material, the excited atomic states enter into the interaction process as virtual

states. In these cases, the nonlinearities of the medium may be generally attributed to the real part of the susceptibility. Since the process is nonresonant, the nonlinear coupling constant is not generally large. And the generated power at the sum or difference frequency is proportional to the product of the two input powers.

Appreciable enhancement of the nonlinear coupling coefficient is expected, however, if the frequencies of the applied fields approach resonances of the material.¹ In these cases both the real and the imaginary parts of the susceptibility play important roles. Additional effects are also encountered when the intensities of the applied

* Work supported by the National Aeronautics and Space Administration.

† On leave of absence from the Weizmann Institute, Rehovot, Israel.

¹ A. Szöke and A. Javan, *Bull. Am. Phys. Soc.* **8**, 381 (1963).

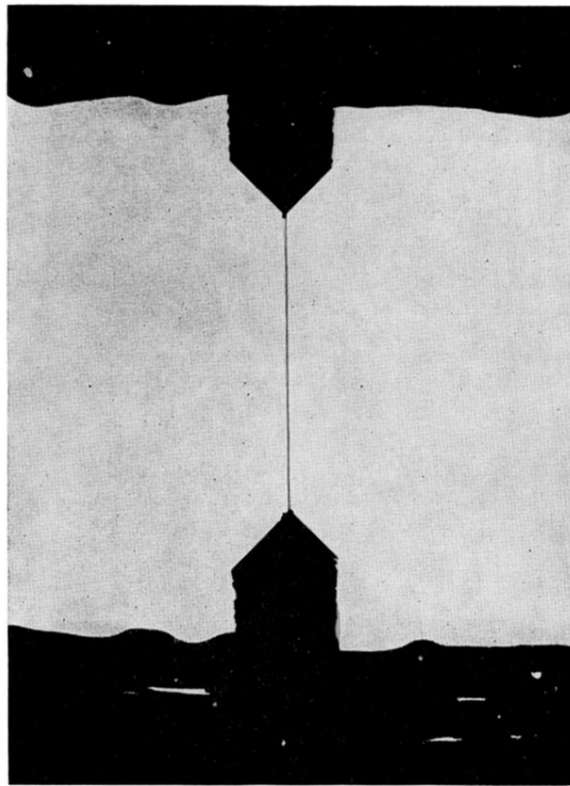


FIG. 4. Microphotograph of specimen.